

Intraday variability in x-ray selected BL Lacertae objects ^{*}, ^{**}

J. Heidt¹ and S. J. Wagner¹

Landessternwarte Heidelberg, Königstuhl,
69117 Heidelberg, Germany

Received 15 July 1997 / Accepted 12 August 1997

Abstract. We present a study of the intraday variability behaviour of two samples of x-ray selected BL Lac objects, the EMSS and EXOSAT samples consisting of 22 and 11 sources, respectively. In both samples we were able to detect intraday variability in less than 40% of the sources only. The duty cycle (the fraction of time, when a BL Lac object is variable) in x-ray selected BL Lac objects is 0.4 or less.

The typical peak-to-peak amplitudes of the variability are 10%. Typical time-scales and an activity parameter for our variable BL Lac objects were inferred from structure function and autocorrelation function analyses. In only 4 BL Lac objects we were able to measure a characteristic time-scale, which was in the range between 1.3 and 2.7 days.

Comparison with our previous study of a complete sample of radio-selected BL Lac objects from the 1 Jy catalogue shows that x-ray and radio-selected BL Lac objects differ in their duty cycle by a factor of 2 and the typical peak-to-peak amplitudes by a factor of 3. The observed time-scales are similar. We also found that the same mechanism may be responsible for the observed variability in the x-ray selected and radio-selected BL Lac objects.

The expectations of the various schemes linking x-ray selected and radio-selected BL Lac objects have been compared to our observations. Consistency is found for a scenario, where x-ray selected BL Lac objects have on average stronger magnetic fields and are seen under relatively larger viewing angles than the radio-selected BL Lac objects. However, the suggestion that x-ray selected BL Lac objects have decelerating jets and radio-selected BL Lac objects accelerating jets can also not be ruled out. In any case, any model which explains variability on time-scales of days must be able to reproduce the high duty

cycle in radio-selected BL Lac objects and the factor of 2 lower duty cycle in x-ray selected BL Lac objects.

Key words: galaxies: active – BL Lacertae objects: general – intraday variability – Methods: statistical

1. Introduction

BL Lac objects are characterised by strong and rapid variability from radio up to γ -rays, high and variable polarization in the radio and optical regime, as well as faint or absent emission lines in their spectra. Additionally, in many sources superluminal motion has been observed. Due to these properties it is nowadays believed that their energy output is dominated by boosted radiation from a relativistic jet pointing almost directly towards the observer. Those objects, whose relativistic jets are pointing more randomly onto the sky are thought to be the Faranoff-Riley I (FR I) radio galaxies (Urry & Padovani, 1995 and references therein).

Whereas the classical BL Lac objects have been identified from radio surveys, most of the newly identified BL Lac objects have been detected in x-ray surveys. These so-called x-ray selected BL Lac objects (XBL) differ from the classical radio-selected BL Lac objects (RBL) in many respects. They have different $\alpha_{\text{RO}} - \alpha_{\text{OX}}$ spectral indices (Stocke et al., 1985) and possibly show different cosmological evolution (Stickel et al., 1991, Morris et al., 1991). Additionally, XBL are not as strongly variable and not as highly polarized in the optical as the RBL (Jannuzi et al., 1993, 1994), they seem to have weaker radio cores and extended emission and are less core dominated (Perlman & Stocke, 1993). On the other hand, no differences have been found among the properties of their host galaxies (Wurtz et al., 1996) and their cluster environment at redshifts below $z = 0.65$ (Wurtz et al., 1997).

Since the detection of “two” classes of BL Lac objects, several suggestions have been made to explain their differences and to unify both classes. Ghisellini et al. (1989, 1993) proposed that XBL and RBL are intrinsically the same objects differing mainly by their average viewing angle of their jets to

Send offprint requests to:

J. Heidt, E-mail: jheidt@lsw.uni-heidelberg.de

* Based on observations collected at the German-Spanish Astronomical Centre, Calar Alto, operated by the Max-Planck-Institut für Astronomie, Heidelberg, jointly with the Spanish National Commission for Astronomy

** Based on observations carried out at the European Southern Observatory, La Silla, Chile during programs N^o 49.B–0036 and N^o 53.B–0036

the observer ($< 30^\circ$ for XBL and $< 15^\circ$ for RBL). Alternatively, Giommi & Padovani (1994) and Padovani & Giommi (1995) suggested that the main difference between XBL and RBL is their spectral energy distribution (SED), where XBL have their cutoff of the synchrotron spectrum at higher frequencies (UV/x-ray regime) than the RBL (near-IR/optical regime). Since they found transition objects (RBL which had their cutoff at higher frequencies and vice versa) they introduced a new classification scheme, the so-called LBL (low-energy cutoff BL Lacs) and HBL (high-energy cutoff BL Lacs). More recently, Sambruna et al. (1996) studied the multifrequency spectral properties of BL Lac objects and explained the differences between XBL and RBL by a systematic change of the intrinsic physical parameters of the jet such that XBL have higher magnetic fields/electron energies and smaller sizes than RBL. Finally, Brinkmann et al. (1996) proposed that XBL and RBL are intrinsically different and either originate from different populations or have emission conditions with different physical parameters (e.g. accelerating jets in RBL and decelerating jets in XBL). In addition to the differences at lower frequencies, RBL turned out to be γ -ray emitters at GeV energies, while all of the TeV emitting BL Lac sources belong to the XBL subtype. If the γ -ray emission is due to inverse Compton scattering, this result confirms that the electron population in XBL is dominated by higher Lorentz factors.

Intraday variability (IDV) measurements of BL Lac objects in the optical are one tool to probe the physics and geometry in the innermost part of the AGN (see Wagner & Witzel, 1995 for a comprehensive summary). Since optical IDV is unaffected by extrinsic effects, such as refractive interstellar scattering, which is important in the radio domain or gravitational microlensing, which might only be important on time-scales of weeks to months, such studies investigate variations intrinsic to the source. With the current availability of medium-sized telescopes in combination with highly efficient CCDs, IDV studies of BL Lac objects as faint as 20mag are possible. This allowed us to observe large samples of BL Lac objects within a reasonable time, with an adequate sampling and with errors lower than in any other frequency regime.

Despite the fact that several groups put major efforts in observing BL Lac objects on time-scales from hours to months (e.g. Fiorucci & Tosti, 1996; Miller & Noble, 1997; Takalo, 1997) the samples observed are mostly chosen on the basis of the brightness of the sources, previously well documented variability, or are restricted to specific objects. In most cases XBL are missing, since only a few are bright enough to be observed with smaller telescopes.

As a consequence, the optical IDV properties of XBL are poorly constrained. Only two XBL - the classical XBL PKS 2155-304 and Mkn 421 - have been the subject of several detailed studies, partly during global multifrequency campaigns (e.g. Carini & Miller, 1992; Courvoisier et al., 1995; Wagner et al., 1997; Pesce et al., 1997; Heidt et al., 1997). These observations showed that XBL have a duty cycle close to unity. However, in PKS 2155-304 also a quiescent period was observed (Heidt et al., 1997). Optical variation on shorter time-scales

(seconds to hours) has been investigated by Miller & Noble (1997) and on longer time-scales by Jannuzi et al. (1993, 1994) and Xie et al. (1996).

In a previous study, we determined the duty cycle, typical amplitudes and time-scales of the complete sample of RBL from the 1 Jy catalogue (Heidt & Wagner, 1996). The duty cycle among the RBL is very high (≈ 0.8), with amplitudes typically reaching 30% and time-scales between 0.5 and 3 days.

Here we present the results of our study of the optical IDV properties of two samples of XBL, the EMSS sample extracted by Morris et al. (1991) and the EXOSAT sample compiled by Giommi et al. (1991). Our goal is to determine the duty cycle, typical amplitudes and time-scales of XBL, to compare our results with those derived from our study of RBL and to interpret our results in view of the competing models linking RBL and XBL.

This paper is organized as follows: In chapter 2 the samples are briefly described, in chapter 3 the observations and the data reduction are summarized. Chapter 4 contains the basic results, the statistical analysis is presented in chapter 5. In chapter 6 we discuss the results of the statistical analysis and compare the results with those derived from our study of RBL followed by the interpretation. Our conclusions are summarized in chapter 7. Throughout the paper $H_0 = 50 \text{ km s}^{-1} \text{ Mpc}^{-1}$ and $q_0 = 0$ is assumed.

2. The x-ray selected samples

2.1. The EXOSAT sample

The EXOSAT sample of BL Lac objects was compiled by Giommi et al. (1991) from the EXOSAT High Galactic Latitude Survey. The 11 objects of this sample were selected using the following criteria:

- Equivalent width of emission lines $< 5 \text{ \AA}$ (rest frame)
- $0.2 < \alpha_{\text{ro}} < 0.55$; $0.6 < \alpha_{\text{ox}} < 1.5$
- x-ray flux (0.05 – 2.0 keV) $> 10^{-12} \text{ ergs cm}^{-2} \text{ s}^{-1}$
- $|b| > 20^\circ$

2.2. The EMSS sample

The EMSS sample of BL Lac objects was extracted by Morris et al. (1991) from the Einstein Medium-Sensitivity Survey. It contains 22 objects, which were selected according to the following criteria:

- Inclusion in the EMSS sample of serendipitous x-ray sources
- Equivalent width of emission lines $< 5 \text{ \AA}$
- Evidence for a non-thermal continuum in the spectra (Ca II break had a contrast of less than 25%)
- x-ray flux (0.3 – 3.5 keV) $> 5 \times 10^{-13} \text{ ergs cm}^{-2} \text{ s}^{-1}$
- $\delta > -20^\circ$

Both samples have one object in common (1207.9+3945). Therefore, this object was observed during two runs. Whereas for the BL Lac objects of the EMSS sample redshifts are available for all sources, only 4 out of 11 BL Lac objects from the

EXOSAT sample have published redshifts. The average redshift of the EMSS BL Lac objects is 0.32. When relevant, we will set a redshift of $z = 0.3$ for all BL Lac objects from the EXOSAT sample, whose redshift is unknown.

3. Observations and data reduction

The observations were carried out during 9 observing runs between September 1992 and April 1995 at the Calar Alto Observatory in Spain, the ESO in Chile and in Cananea, Mexico. The telescopes were equipped with a CCD and an R filter in order to perform relative photometry. An overview about the observing runs is given in Table 1.

Table 1. Observing journal

Observatory	Period
ESO, Danish 1.5m	September 1992
Calar Alto, 2.2m	February 1993
Calar Alto, 2.2m	May 1993
Calar Alto, 2.2m	March 1994
Cananea, 2.1m	April 1994
ESO, Danish 1.5m	July 1994
Calar Alto, 2.2m	August 1994
Calar Alto, 2.2m	December 1994
Cananea, 2.1m	April 1995

In order to create a homogeneous dataset we tried to observe each BL Lac object during seven consecutive nights with an average sampling rate of 2 hours. Due to various circumstances (weather, technical problems etc.), however, the sampling and the length of our data trains for the two samples are different.

Each BL Lac object of the EXOSAT sample was observed on average 2-3 times per night during 7 nights. Apart from EXO 1146+2455, which could be observed during 3 nights only, each object was observed at least during 5 nights. About 50% of the EXOSAT BL Lacs have been observed at least during 10 nights.

Our observations of the EMSS BL Lacs were more densely sampled. Most of the sources have been observed 4-5 times per night for a period of 6 nights, the shortest data train was 5 nights, with a sampling of once per night (MS 0922.9+7459 and MS 1534.2+0148). About 25% of the sources were observed during at least 9 nights (c.f. Table 2).

The integration times varied between 5 and 30 minutes depending on the brightness of the BL Lac object, the observing conditions and the size of the telescope. They were chosen such that the signal to noise in the central pixel of the BL Lac object was as high as possible but the count rate approximately 30% below the saturation limit or the non-linearity limit and

the count rates of the comparison stars varied no more than a factor of two within each campaign.

The CCD frames were reduced in a standard manner (bias subtracted, corrected for dark current, if necessary, pixel-to-pixel variations removed using twilight flat-fields).

In order to carry out relative photometry the count rates of the BL Lac object and 5 to 10 comparison stars were measured on each frame by simulated aperture photometry. We computed the normalized ratio for each pair of objects over the entire campaign to construct lightcurves. By inspecting the lightcurve of each pair, variable stars were found and rejected from further analysis. For the final analysis the lightcurves were used which included the BL Lac object and the brightest, non-saturated comparison star. The errors were estimated from the standard deviation (1σ) of the lightcurve of two comparison stars as bright as or fainter than the BL Lac object. They are typically in the order of 0.6-2%, in worst cases up to 5% (corresponding to 0.06mag).

4. Variability statistics and amplitudes

In order to derive the number of BL Lac objects displaying variability during the observations we applied a χ^2 -test following Penston & Cannon (1970) to each lightcurve. As in our study of the radio-selected BL Lac objects from the 1 Jy sample (Heidt & Wagner, 1996) we choose a confidence level of 99.5% as cutoff. The χ^2 -test was carried out twice. First we applied this test to all lightcurves. This gave us the fraction of the variable and the non-variable BL Lac objects. Since we were interested in variability time-scales from several hours to one week, we subtracted trends on longer time-scales by fitting a linear slope to each lightcurve of the variable objects. After subtraction of these slopes, the χ^2 -test was applied to the residuals.

6 out of the 11 BL Lac objects from the EXOSAT sample displayed variability during the observations, corresponding to a fraction of 55%. In only 4 out of the 11 sources (36%) we were able to detect intraday variability. The fraction of variable EMSS BL Lac objects was lower. Here we could detect variability in only 7 out of 22 BL Lac objects (32%), 6 out of this 7 showed intraday variability (corresponding to 27% for the EMSS sample). In Table 2 we list the both samples along with their average R band magnitude during the observations, their redshift, the number of observations, the maximum time separation between two observations and in column 6 the results of the χ^2 -tests for a confidence level of 99.5%. A ++ sign denotes the intraday variable, a + sign variable, but on time-scales longer as the observing period and a – sign the non-variable BL Lac objects. For comparison we give the confidence of the χ^2 -test to the residuals after subtraction of a linear slope from the lightcurves in column 7. The final two columns list the variability amplitudes as defined below as well as the measurement error and information about the observing period and telescope used.

We checked, whether a lower confidence level, e.g. 90% as used by Penston & Cannon (1970), would alter the distribution. We ran through the χ^2 procedure for the lower cutoff limit

as outline above. Whereas we found no change in the classification of the BL Lac objects from the EXOSAT sample, the number of variable EMSS BL Lac objects increased. Now, 15 out of 22 EMSS BL Lac objects (68%) would be classified as variable, 8 of them (36%) would display intraday variability.

Regardless of the cutoff limit used, we conclude that less than 40% of all x-ray selected BL Lac objects from our samples displayed intraday variability during the observations.

In order to test, if the variability amplitudes are correlated with the average brightness of the objects, we calculated the variability amplitudes $Amp = \sqrt{(A_{max} - A_{min})^2 - 2\sigma^2}$ where A_{max} and A_{min} are the maximum and minimum values of each lightcurve and σ the measurement errors, respectively. They are given for each individual object in Table 2 in column 7.

The mean amplitude for the intraday variable EXOSAT sources is $9.0 \pm 3.8\%$, for the intraday variable EMSS sources $10.6 \pm 4.5\%$. Including also the sources variable on longer time-scales, the mean amplitude for the variable EXOSAT sources is $8.8 \pm 3.1\%$ and for the variable EMSS sources $10.0 \pm 4.3\%$.

In Figure 1 we plot the average brightness of the BL Lac objects during the observations against the variability amplitudes. For comparison we have also included the "variability amplitudes" of the non-variable sources. Obviously, there is no correlation between variability amplitudes and average brightness.

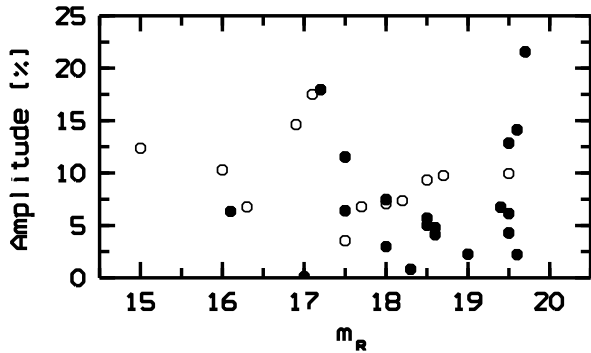


Fig. 1. Variability amplitudes versus average brightness. The circles correspond to the variable, the dots to the non-variable sources.

5. Temporal characteristics of the variability

The temporal characteristics of the variability have been studied using two statistical methods, structure function analysis and autocorrelation function analysis. Structure function analysis is a powerful tool to measure time-scales from the lightcurves, especially when the data sampling is rather inhomogeneous. Additionally, determining the slopes of the structure function allows to characterize the underlying physical process. The autocorrelation analysis was used to derive typical amplitudes per time interval. Since we described the ap-

plication of both methods for our study of the 1 Jy sample of BL Lac objects in detail (Heidt & Wagner, 1996), we will here only shortly summarize our adopted strategy.

First order structure functions (SF) were calculated from the lightcurves according to Simonetti et al. (1985). The first order structure function is defined as:

$$SF(\Delta t) = \frac{1}{N} \sum_{i=1}^N (f(t_i + \Delta t) - f(t_i))^2 \quad (1)$$

The power α of $SF \propto (\Delta t)^\alpha$ characterizes the variability and hence the underlying process. If $\alpha = 1$ shot noise dominates, towards flatter slopes ($\alpha = 0$) flicker noise becomes more important (Smith et al., 1993). Characteristic time-scales show up as maxima in the SF (Wagner et al., 1996). Since we were interested mainly on the characteristics of the variability on short time-scales and since we wanted to compare our results to those derived for the 1 Jy BL Lac objects, we decided to study the $SF(\Delta t)$ within the time interval $0.5 \text{ days} < \Delta t < 5 \text{ days}$. As in Heidt & Wagner (1996) we binned the SF in variable intervals such that each interval contains the same amount of differences $\Delta I(t_1, t_2)$ with $t_2 < t_1$, where the number of bins depends on the total number of data points n .

The autocorrelation function (ACF) of each variable object was computed following the discrete correlation function method described by Edelson & Krolik (1988). As in the case of the structure function analysis, we had to deal with a rather inhomogeneous sampling. Therefore our binsize Δt was chosen to be 0.2 or 0.5 days, depending on the evenness of the measurements between and during the nights (see Heidt & Wagner, 1996, section 5.2 for details).

5.1. Slopes and characteristic time-scales measured from the SF

The slopes α of the SF were measured by fitting a 1st order polynomial using the least-squares method to the SF in the $\log(SF) - \log(\Delta t)$ plane. Slopes were determined only in those SF, which had at least three bins in the range between 0.5 and 5 days. This was possible for all 13 variable sources except MS 1757+7034, where the "best fit" was not acceptable. The resulting slopes are given in Table 3. They range from -0.6 to 1.6, with a mean value of 0.8 and a dispersion of 0.7. The two sources with negative slopes (EXO 1215.3+3022 and MS 1229.2+6430) are dominated by rapid variability on time-scales around one day. Their structure functions are shown in Figure 2.

For two sources of each sample, we were able to measure a characteristic time-scale by identifying pronounced maxima in the $\log(\Delta t) - \log(SF)$ plane. These are EXO 1004.0+3509, EXO 1215.3+3022 as well as MS 1221.8+2452 and MS 1402.3+0416. All sources show similar intrinsic time-scales between 1.3 and 2.7 days.

Table 2. The x-ray selected samples

Object	m_R	z	n	dt [days]	χ^2	Confidence [%]	Amplitude [%]	Date/Telescope
The EXOSAT sample								
EXO 0556.4–3838	17.5		18	5.20	++	99.6	3.5(0.6)	09/92 (ESO,1.5)
EXO 0706.1+5913	17.0	0.125	13	9.87	–	0.01	0.1(1.2)	03/93 (CA,2.2)
EXO 0811.2+2949	18.5		11	9.80	+	0.01	9.3(1.2)	03/93 (CA,2.2)
EXO 1004.0+3509	19.5		13	9.88	++	99.9	9.9(1.5)	03/93 (CA,2.2)
EXO 1118.0+4228	18.0		13	9.90	–	79.0	7.5(2.5)	03/93 (CA,2.2)
EXO 1146.9+2455	19.0		8	2.12	–	5.6	2.3(1.5)	03/93 (CA,2.2)
EXO 1207.9+3945	20.0	0.615	9	10.00	–	3.8	2.2(1.8)	03/93 (CA,2.2)
EXO 1215.3+3022	16.0		19	5.12	++	100.0	10.2(1.3)	05/93 (CA,2.2)
EXO 1218.8+3027	15.0		29	9.16	++	100.0	12.3(0.9)	01/92 (CA,1.2)
EXO 1415.6+2557	17.5	0.237	23	6.16	–	34.1	6.5(1.0)	05/93 (CA,2.2)
EXO 1811.7+3143	18.0	0.117	22	5.18	+	3.6	7.1(1.3)	05/93 (CA,2.2)
The EMSS sample								
MS 0122.1+0903	19.5	0.339	25	5.28	–	64.9	6.1(1.7)	12/94 (CA,2.2)
MS 0158.5+0019	18.5	0.299	15	4.20	–	45.0	5.0(1.5)	09/94 (ESO,1.5)
MS 0205.7+3509	18.6	0.318	33	5.33	–	4.5	4.8(1.5)	12/94 (CA,2.2)
MS 0257.9+3429	18.0	0.247	35	5.36	++	99.7	7.4(1.1)	12/94 (CA,2.2)
MS 0317.0+1834	17.7	0.190	37	5.36	+	63.8	6.8(1.1)	12/94 (CA,2.2)
MS 0419.3+1943	19.7	0.512	36	5.38	–	87.7	21.6(4.0)	12/94 (CA,2.2)
MS 0607.9+7108	18.2	0.267	24	4.35	–	97.0	7.4(2.5)	03/94 (CA,2.2)
MS 0737.9+7441	18.0	0.315	24	4.33	–	0.01	3.0(1.2)	03/94 (CA,2.2)
MS 0922.9+7459	19.5	0.638	5	4.08	–	93.5	4.3(1.0)	03/94 (CA,2.2)
MS 0950.9+4929	18.6	0.207	22	4.29	–	89.7	4.1(1.0)	03/94 (CA,2.2)
MS 1207.9+3945	19.6	0.615	7	5.92	–	49.4	14.1(5.0)	04/94 (Can,2.1)
MS 1221.8+2452	17.1	0.218	23	4.28	++	100.0	17.5(1.2)	03/94 (CA,2.2)
MS 1229.2+6430	16.3	0.164	23	4.29	++	100.0	6.8(0.6)	03/94 (CA,2.2)
MS 1235.4+6315	18.5	0.297	17	6.06	–	6.9	5.6(2.5)	04/94 (Can,2.1)
MS 1402.3+0416	16.9	0.200	19	4.23	++	100.0	14.6(0.8)	03/94 (CA,2.2)
MS 1407.9+5954	19.4	0.495	24	9.10	–	76.9	6.7(1.5)	08/94 (CA,2.2)
MS 1443.5+6349	19.5	0.299	22	8.07	–	88.8	12.8(2.9)	08/94 (CA,2.2)
MS 1458.8+2249	16.1	0.235	16	4.19	++	99.5	6.3(0.7)	08/94 (CA,2.2)
MS 1534.2+0148	18.3	0.312	5	3.98	–	5.4	0.8(0.8)	04/94 (Can,2.1)
MS 1552.1+2020	17.2	0.222	25	7.23	–	24.4	17.9(4.0)	04/94 (Can,2.1)
MS 1757.7+7034	18.7	0.407	34	9.16	++	99.9	9.7(1.5)	08/94 (CA,2.2)
MS 2143.4+0704	17.5	0.237	33	9.16	–	74.7	11.5(2.0)	08/94 (CA,2.2)

Column 1 gives the name of the sources, column 2 the average brightness (m_R) during the observations and column 3 the redshift. In column 4 the number of observations are listed, in column 5 the maximum time separation between two observations and in column 6 the result of the χ^2 -tests. A ++ sign denotes the intraday variable, a + sign variable, but on time-scales longer than the observing run and a - sign the non-variable sources (see text for details). The confidence of the χ^2 -test to the residuals after subtraction of a linear slope from the lightcurves is given in column 7. Column 8 contains the variability amplitude as defined in the text. Here the 1σ errors are included in brackets. Column 9 finally gives the observing dates, the observatory and the telescope used. ESO, 1.5 = ESO Danish 1.5m; CA, 2.2, 1.2 = Calar Alto 2.2m, 1.2m, and Can, 2.1 = Cananea 2.1m, Mexico, respectively.

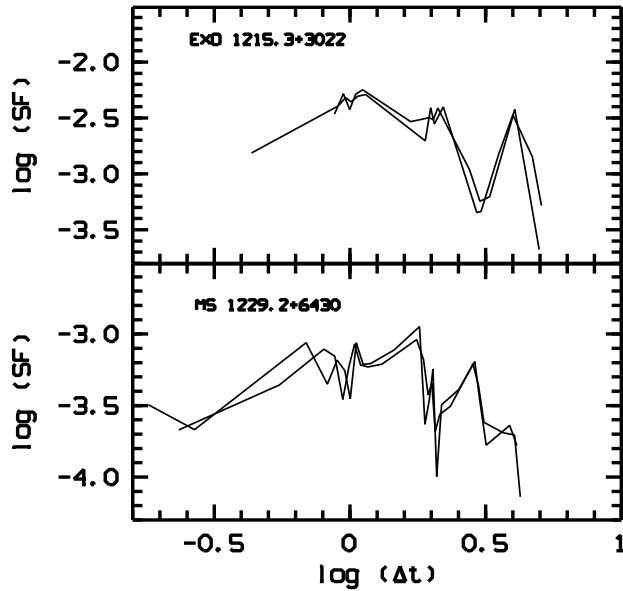


Fig. 2. Structure functions of EXO 1215.3+3022 (top) and MS 1229.2+6430 (bottom). Both sources are dominated by rapid variability on time-scales around one day. This results in negative slopes in the range between 0.5 and 5 days.

Object	Slope α	Δt [days]	\dot{I} [%/day]
EXO 0556.4–3838	0.59(.12)		0.32(.49)
EXO 0811.2+2949	1.55(.26)		0.37(.91)
EXO 1004.0+3509	1.42(.48)	2.7(.27)	0.85(.85)
EXO 1215.3+3022	-0.29(.13)	1.3(.14)	2.25(.66)
EXO 1218.8+3027	0.59(.08)		0.86(.96)
EXO 1811.7+3143	1.44(.22)		0.36(.57)
MS 0257.9+3429	0.55(.14)		1.14(.47)
MS 0317.0+1834	0.92(.19)		
MS 1221.8+2452	0.38(.15)	2.4(.25)	4.94(1.82)
MS 1229.2+6430	-0.63(.17)	2.7(.25)	2.17(.66)
MS 1402.3+0416	1.21(.12)		2.89(2.04)
MS 1458.8+2249	1.44(.11)		1.69(.38)
MS 1757.7+7034			1.09(.18)

Table 3. Results of the statistical analyses of the variable BL Lac objects. Column 1 gives the name of the sources, column 2 the slopes α of the SF, column 3 the time-scales found from the SF and column 4 the activity parameter \dot{I} measured from the ACF. 1σ errors are given in brackets. The time-scales and activity parameter have been corrected for cosmological effects.

5.1.1. The activity parameter \dot{I} from the autocorrelation function analysis

Since we want to measure a typical amplitude per time interval of a BL Lac object, we calculated the activity parameter $\dot{I} = \sqrt{\text{ACF}(0)/\Delta t}$ from the ACF by fitting a 2nd order polynomial to the ACF of each variable object. Therefore the ACF was not normalized to unity at $\Delta t = 0$. ACF(0) and Δt were derived from the maximum and the decorrelation length of the fit parabola. With the exception of MS 0317.0+1834 we could determine \dot{I} for all variable BL Lac objects. The results are given in Table 3 in column 4. Except MS 1221.8+2452, which had an \dot{I} of $\approx 5\%$ /day, all variable BL Lac objects displayed a moderate variability of 3%/day or less.

6. Discussion

6.1. IDV properties of the XBL

Our observation show that only 6 out of 22 (27%) of the EMSS XBL and 4 out of 11 (36%) EXOSAT XBL displayed IDV. Using a less restrict definition of IDV (cutoff limit 90% for the χ^2 test) now 8 out of 22 (36%) EMSS XBL would be classified as IDV, the number of EXOSAT XBL displaying IDV would not change. Altogether, we conclude that the detection rate is less than 40%. Under the assumption that this detection rate can be transformed to a duty cycle (the fraction of time, when a BL Lac is variable), the duty cycle in XBL would be 0.4 or less.

To our knowledge no systematic study of the IDV behaviour of XBL have been carried out so far. It is hence difficult to compare the results obtained with other studies. Xie et al. (1996) observed 6 EMSS and 1 EXOSAT XBL during the last years with an irregular sampling, from hours to months. All sources have been observed occasionally several times per night during two or three subsequent nights. In 5 of the 7 sources they found IDV with amplitudes between 0.3 and 0.5mag on time-scales from hours to 2 days. In 3 out of these 5 sources (EXO 1218.8+3027, MS 0317+1834, MS 1402.3+0416) we found also IDV, but no XBL of our samples displayed as large variability amplitudes as found by Xie et al. (1996). We found mean amplitudes of $\approx 10 \pm 4\%$ in both samples, the most extreme case being MS 1221.8+2452 with an amplitude of 17.5%. However, the strong variability amplitudes observed by Xie et al. (1996) depend in all cases on one single data point in their lightcurves only, so their results must be regarded as uncertain.

Optical photometry and polarimetry on longer time-scales (weeks to month) of 37 XBL have been presented by Januzzi et al. (1993, 1994). Their sample includes 21 of the EMSS XBL (except MS 1443.5+6349) and one EXOSAT XBL (EXO 1415.6+2559). In spite of the faintness of some sources, which made variability measurements impossible, they detected variability in 12 out of this 22 sources, with amplitudes of always less than 1mag. The “duty cycle” on time-scales from weeks to month of this sample would be ≈ 0.55 , which is slightly higher as our duty cycle of 0.4. It is interesting to note that their duty

cycle of optical polarization (fraction of the time, where a BL Lac shows polarization $> 4\%$) of their sample of 37 objects is ≈ 0.4 .

Optical Variations of 12 XBL on shorter time-scales (seconds to hours) have been studied by Miller & Noble (1997). They found a duty cycle of ≈ 0.8 for the XBL they observed, which is a factor of two higher as derived from our study on longer time-scales. However, they do neither quote their sources nor their selection criteria such that a direct comparison is not possible.

From our structure function analysis we could derive characteristic time-scales for 4 XBL only, which corresponds to a fraction of 12%. They were in the range between 1.3 and 2.7 days. The slopes of the SF range from -0.6 up to 1.6 with a mean of 0.8 ± 0.7 indicating that in these sources shot noise is the most dominating process. From our autocorrelation function analysis we could measure a typical amplitude per time interval for all variable sources except MS 0317.0+1834. In all but one source (MS 1221.8+2452) we derived an \dot{I} of 3%/day which indicates that our XBL show on average modest variability only.

Two prominent XBL - the classical XBL PKS 2155-304 and Mkn 421 - were subject to several multifrequency campaigns during the last years (e.g. Carini & Miller, 1992; Courvoisier et al., 1994; Wagner et al., 1997; Pesce et al., 1997; Heidt et al., 1997). Whereas the observations generally have shown that in both XBL the duty cycle in the optical on time-scales of days is close to unity, in PKS 2155-304 also a quiescent period was observed (Heidt et al., 1997). Both objects occupy the region typical for XBL in the $\alpha_{RO} - \alpha_{OX}$ diagram, however, they are unusually bright in the radio, optical and x-ray domain. Both XBL may be an extreme member of its class.

We checked for any dependences of the time-scales, amplitudes or the activity parameter \dot{I} on intrinsic properties such as absolute magnitude or redshift and found none.

6.2. IDV properties of XBL compared to RBL

We compare now our results of the IDV properties of XBL to those derived in our study of the 1 Jy RBL sample (Heidt & Wagner, 1996).

In Figure 3 we compare the variability statistics of the EMSS sample, the EXOSAT sample and the 1 Jy sample. Note the clear difference on the number of BL Lacs showing IDV, variability on time-scales longer than an observing run (typically 7 days) and non-variable sources between XBL and RBL. This diagram shows that the rate of occurrence of IDV in both classes is different. For our XBL we determined a duty cycle of ≈ 0.4 , whereas a duty cycle of at least 0.8 was found for the RBL. We checked whether IDV is a coincidence in RBL by repeated observations of various subsamples of the 1 Jy sample and found always a duty cycle around 0.8 (Wagner et al., 1990; Bock, 1994). The duty cycle on time-scales of days differs between both classes at least by a factor of 2.

In order to quantify the difference of the rate of occurrence of IDV between RBL and XBL we performed a KS-test to the

results of the χ^2 distribution (see section 4). We found a probability of $\sim 2 \times 10^{-6}$ that the distributions of the χ^2 have been drawn from the same parents.

Miller & Noble (1997) determined the duty cycle of 12 XBL and 20 RBL. They found no difference between both classes on shorter time-scales (seconds to hours). However, they do neither quote their sources nor their selection criteria. This is critical for such a comparison. Obviously, the apparent discrepancy could be understood, if the samples of Miller & Noble consisted mainly of XBL and RBL, which were already known to be very active.

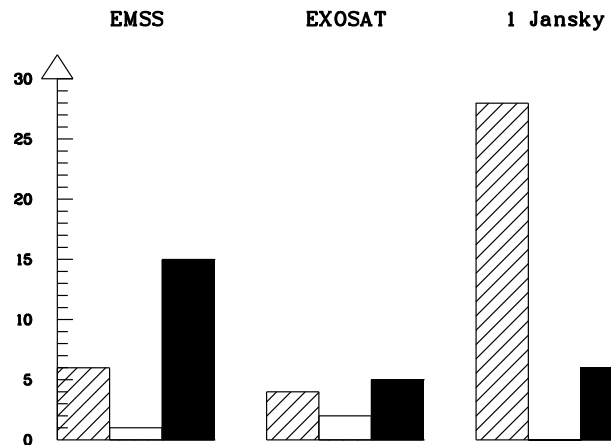


Fig. 3. Histogram showing the distribution of the sources showing IDV (shaded), the sources variable only on time-scales longer than the observing run (open) and the non-variable sources (black) among our three samples observed. Note the clear difference in the distribution between the XBL (EMSS, EXOSAT) and RBL (1 Jansky).

We also find significant differences in mean amplitudes between XBL and RBL. For the intraday variable XBL we determined a mean amplitude of $10.0 \pm 4.1\%$ whereas we found mean amplitudes of $28.2 \pm 19.7\%$ for the variable RBL. The amplitudes in XBL and RBL differ by a factor of three as illustrated in Figure 4. This confirms that RBL also tend to have higher amplitudes on average than XBL in Miller & Nobles microvariability study.

The distribution of the activity parameter \dot{I} (amplitude per time interval) seems to differ among both classes. Whereas the variable RBL showed a wide range of \dot{I} up to 27%/day, the variable XBL had an \dot{I} of 3%/day or less (except MS 1221.8+2452 with an \dot{I} of $\approx 5\%$ /day). This is shown in Figure 5, where we compare the distribution of the \dot{I} found among the XBL and RBL.

There also seems to be a difference between both classes when correlating \dot{I} with the absolute magnitude of the sources. Whereas we found a trend for higher \dot{I} towards higher M_R in RBL, there is no such trend for the XBL as can be seen in Figure 6a. However, high luminosity XBL are missing in our diagram. In order to test, whether this trend is already present

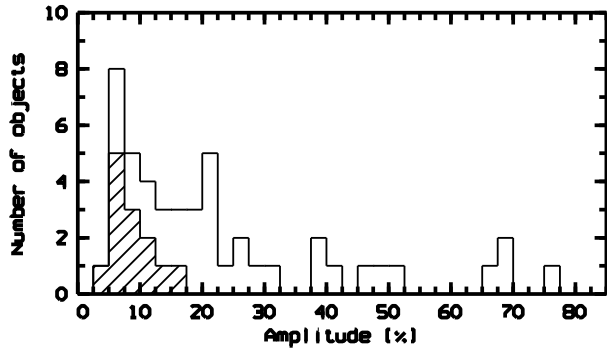


Fig. 4. Histogram of the amplitudes of the variable XBL (shaded) and variable RBL (open). The difference in amplitudes can clearly be seen.

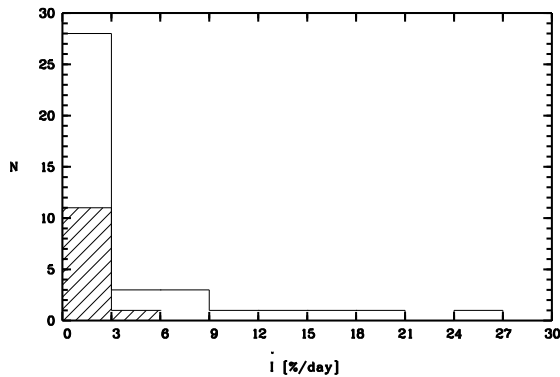


Fig. 5. Histogram with the distribution of the \dot{I} for XBL (shaded) and RBL (open).

in low-luminosity sources, we performed a KS-test on the distribution of the \dot{I} for the XBL and RBL with $M_R > -27$. The cumulative distributions are shown in Figure 6b. The KS-test gave a probability of 92.5% that the two distributions are drawn from the same parent population. As long as no information on high-luminosity XBL is available, we cannot decide, whether only RBL show a trend of higher \dot{I} towards higher M_R or the observed trend reflects two intrinsically different types of objects.

In only 4 XBL displaying IDV we could measure a typical time-scale of the variations from our structure function analysis. The range found (1.3–2.7 days) was similar to that derived from the 1 Jansky sample of RBL (0.5–3 days).

The average slopes α of the SF of both classes are similar (0.8 ± 0.7 for XBL and 0.8 ± 0.6 for RBL), implying that the same mechanism might be responsible for the observed variability in both classes of BL Lac objects.

Finally, neither class shows a dependence of the amplitudes or time-scales on intrinsic properties (e.g. redshift, absolute magnitude).

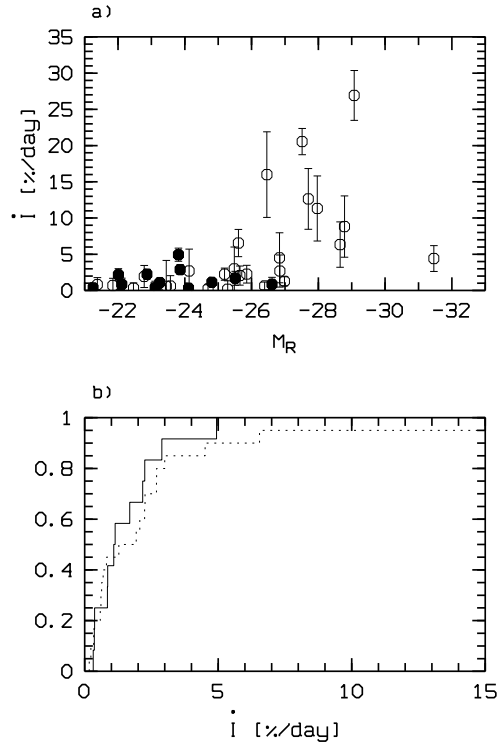


Fig. 6. a) Activity parameter \dot{I} versus absolute magnitude M_R . The dots correspond to XBL, the open circles to RBL. The amplitudes and time-scales involved in the derivation of \dot{I} have been corrected for cosmological effects. b) Cumulative distributions of the \dot{I} for XBL (solid) and RBL (dashed) having $M_R > -27$. The KS-test gave a probability of 92.5% that the two distributions have been drawn from the same parent population.

6.3. Are XBL and RBL intrinsically different?

Our study of the IDV properties of XBL and RBL has shown that both classes differ in many respects. The duty cycle differs by a factor of ≈ 2 , the variability amplitudes by a factor of ≈ 3 . Additionally, the typical amplitudes per time interval are moderate in XBL, whereas a fraction of RBLs show also stronger amplitudes per time interval. On the other hand, we found similar time-scales and slopes from the structure function analysis among both classes indicating that the same mechanism is responsible for the observed variability. In the following we will compare these results to the expectations based on the various suggestions linking both classes of AGN.

Ghisellini & Maraschi (1989) and Ghisellini et al. (1993) explained the observed different overall spectral shapes of XBL and RBL by a different viewing angle between the relativistic jet axes and the observer. Their model is based on the assumption that the x-ray emission comes from more closely to the base of the jet and is more isotropic than the radio emission, which originates further away from the baseline and is more strongly beamed. They conclude that RBL should be seen under an inclination angle $\theta < 15^\circ$ and the XBL under an inclination angle $\theta < 30^\circ$. With this assumption and a Doppler

factor δ scaling as $\sim 1/\sin\theta$ one would expect higher amplitudes, shorter timescales and a higher activity parameter $\dot{\Gamma}$ of the RBL as compared to the XBL. This is confirmed by our results. However, based on their model, one would expect a similar duty cycle among both classes, which we did not find. Therefore orientation effects can not account for the observed IDV properties alone.

Alternatively, Giommi & Padovani (1994) and Padovani & Giommi (1995) argued that a classification of BL Lac objects into XBL and RBL is based rather on the identification in the corresponding frequency band as a physical distinction. They proposed a new classification scheme, the so-called LBL (low-energy cutoff BL Lacs) and HBL (high-energy cutoff BL Lacs), where the LBL have the high-energy cutoff of their synchrotron spectra somewhere in the IR-optical and the HBL somewhere in the UV/x-ray regime. Although most of the XBL are classified as HBL and most RBL as LBL there are transition objects (XBL, which are classified as LBL and vice versa). In this scenario simple predictions of IDV characteristics can be made: since the spectral slope of the LBL is steeper at optical frequencies as compared to the HBL one would expect stronger amplitudes, similar time-scales and a higher activity parameter $\dot{\Gamma}$ for the LBL as compared to the HBL but a similar duty cycle for LBL and HBL.

In order to compare these predictions with our results, we sorted our BL Lacs observed in LBL and HBL. All 11 EXOSAT and 22 EMSS BL Lacs are HBL and all 34 1 Jy BL Lacs except Mkn 501 and PKS 2005-489, which are classified as HBL are LBL (Padovani, priv. communication), i.e. we have now 35 HBL and 32 LBL. The LBL show indeed stronger amplitudes, similar time-scales and a higher activity parameter $\dot{\Gamma}$ as the HBL. However, now 12 out of 35 HBL show IDV, corresponding to a fraction of <40% and 26 out of 32 LBL show IDV corresponding to a fraction of 80%. The duty cycle among both classes still differ by a factor of 2. Therefore the different high-energy cutoff among both classes cannot account for the different duty cycle.

More recently, Sambruna et al. (1996) proposed a systematic change of the intrinsic jet parameters as an explanation for the observed different global spectra of XBL and RBL. They investigated the multifrequency spectral properties of the complete EMSS sample, 29 1 Jy BL Lacs and a complete sample of flat spectrum radio quasars (FSRQ) from the S5 survey, which have all been observed by ROSAT in pointed mode. By computing composite $\alpha_{\text{ox}} - \alpha_x$ spectra for which positive or negative values indicate concave or convex spectra, respectively, they found that the EMSS XBL tend to have convex spectra, the FSRQ concave spectra and the 1 Jy RBL a mixture of both.

Based on their results they fitted homogeneous and inhomogeneous (accelerating) jet models to three representative (convex, concave and intermediate $\alpha_{\text{ox}} - \alpha_x$) multifrequency spectra and concluded that a different viewing angle (beaming factor) can not account for the observed global spectra alone, but requires instead a systematic change of intrinsic jet parameters such as magnetic fields, maximum electron energy or jet size. The change should be such that objects having convex

spectra have stronger magnetic fields, higher electron energies and smaller sizes of their jets as objects having concave spectra.

In order to see, whether there is any trend of the shape of the composite spectra with our IDV properties derived, we correlated their $\alpha_{\text{ox}} - \alpha_x$ with our amplitudes and $\dot{\Gamma}$, but found no correlation. We also calculated the mean $\alpha_{\text{ox}} - \alpha_x$ for our variable and non-variable BL Lacs from the EMSS and 1 Jy sample and found an $\overline{\alpha_{\text{ox}} - \alpha_x} = 0.13 \pm 0.61$ for the variable sources and an $\overline{\alpha_{\text{ox}} - \alpha_x} = -0.24 \pm 0.49$ for our non-variable sources. This shows that the IDV properties are independent of $\alpha_{\text{ox}} - \alpha_x$.

Nevertheless, their scenario is appealing since it could reproduce all of the IDV properties. Under the assumption that IDV is most likely originating from perturbances within a relativistic jet it might be possible that a varying jet configuration such as stronger magnetic fields in the jet of XBL would be more resistant against such perturbances. This could explain the different duty cycle between XBL and RBL. Additionally, a different average viewing angle and hence different beaming factors could also explain the different variability amplitudes.

Different conclusions for the relationship between RBL and XBL were drawn by Brinkmann et al. (1996). They favor a scenario, where either RBL have accelerating and XBL decelerating jets or XBL are intrinsically less beamed BL Lac objects. Their conclusions were drawn from a multi-frequency study of a large number of RBL, XBL and highly polarized quasars (HPQ), which have been observed with ROSAT. By comparing the x-ray and radio fluxes, the relations between x-ray and radio luminosity and by correlating the flux ratios $f_{\text{x-ray}}/f_{\text{radio}}$ and $f_{\text{optical}}/f_{\text{radio}}$ of these three classes they found indications that RBL and XBL are two intrinsically different types of BL Lac objects.

Whereas the scenario that XBL are intrinsically less beamed objects can not explain our results (see discussion above), the alternative scenario that RBL have accelerating jets and XBL have decelerating jets does not provide unique predictions on IDV. Additionally, the IDV properties of RBL are poorly constrained in x-rays (Heidt et al., in preparation) and unknown for XBL in the radio domain.

Obviously, the main problem for all the models discussed above is the different duty cycle between RBL and XBL. One possibility to avoid this difficulty could be that most non-variable XBL show IDV but below our detection limit. However, than there must be a class of BL Lac objects which have variability amplitudes a factor of 10-20 lower as compared to a typical XBL (0.5-1% versus $\sim 10\%$). This can hardly be tested with the current observing techniques.

Although several models linking RBL and XBL have been suggested in the last years, none of them can fully explain the observational facts. This applies also for our observations. Why the duty cycle among RBL and XBL differs by a factor of two has still not been answered, especially since the physical mechanism causing variability is most likely the same in both classes. Within the shock in jet model by Marscher & Gear (1985) the duty cycle can be transformed in a number of shocks

travelling along a relativistic jet. Different duty cycles require a mechanism, which injects these shocks with a different injection rate.

7. Conclusions

We have studied the variability behaviour of the the EMSS and EXOSAT samples of XBL on time-scales of days. Our results can be summarized as follows:

- In 4 out of 11 EXOSAT sources (36%) and in 6 out of 22 EMSS sources (27%) we were able to detect variability on time-scales of days or less. This implies that the duty cycle in XBL is 0.4 or less.
- In only 4 BL Lac objects we could measure a typical time-scales, which was in the range of 1.3-2.7 days.
- The typical peak-to-peak amplitudes of the variability were $\sim 10\%$.
- We investigated an activity parameter \dot{I} from the variable BL Lac objects. All but one BL Lac displayed an \dot{I} of 3%/day or less.

Comparison with our study of the complete sample of RBL from the 1 Jy catalogue shows that the duty cycle between XBL and RBL differs by a factor of two, the typical peak-to-peak amplitudes by a factor of three. Whereas the RBL showed a wide range of \dot{I} up to 27%/day, all but one XBL had an \dot{I} of 3%/day or less. In both classes we found similar time-scales of the variability. We also found similar slopes from our structure function analysis for both classes. This implies that the same process is responsible for the observed variability. No correlation of the variability amplitudes or time-scales with intrinsic properties have been detected in both classes.

We compared our results with the various suggestions linking RBL and XBL. While we can rule out pure inclination effects or the different high-energy cutoff of the synchrotron tail as being responsible for our observed differences, a combination of varying jet configuration (e.g. stronger magnetic fields in the jets of XBL as compared to the RBL) and a different average viewing angle might explain our observations. A scenario, where RBL have accelerating and XBL decelerating jets can not be tested with our observations. Nevertheless, every model explaining variability on time-scales of days must take into account the high duty cycle in RBL and the factor of 2 lower duty cycle in XBL.

Acknowledgements. The authors would like to thank H. Bock, A. Heines and A. Sillanpää for assistance during the observations and Drs. M. Camenzind and A. Witzel for valuable and stimulating discussions. Special thanks to Dr. K. Birkle for his permission to use a few test nights at the Calar Alto 2.2m telescope as well as the Calar Alto OPC for the generous allocation of telescope time during the course of the whole project. This work was supported by the DFG (Sonderforschungsbereich 328).

References

Bock H., 1994, Master thesis, University of Heidelberg

- Brinkmann W., Siebert J., Kollgaard R.I., Thomas H.-C., 1996, A&A 313, 356
- Carini M.T., Miller H.R., 1992, ApJ 385, 146
- Courvoisier T.J.-L., Blecha A., Bouchet P., et al., 1995, ApJ 438, 108
- Edelson R.A., Krolik J.H., 1988, ApJ 333, 646
- Fiorucci M., Tosti G., 1996, A&AS 117, 475
- Ghisellini G., Maraschi L., 1989, ApJ 340, 181
- Ghisellini G., Padovani P., Celotti A., Maraschi L., 1993, ApJ 407, 65
- Giommi P., Tagliaferri G., Beuermann K., et al., 1991, ApJ 378, 77
- Giommi P., Padovani P., 1994, MNRAS 268, L51
- Heidt J., Wagner, S.J., 1996, A&A 305, 42
- Heidt J., Wagner S.J., Wilhelm-Erkens U., 1997, A&A, in press
- Jannuzi B.T., Smith P.S., Elston R., 1993, ApJS 85, 265
- Jannuzi B.T., Smith P.S., Elston R., 1994, ApJ 428, 130
- Marscher A.P., Gear W.K., 1985, ApJ 298, 114
- Miller H.R., Noble, J.C. 1997, The microvariability of Blazars and related AGN. In: Miller H.R., Webb J.R., J.C. Noble (eds.) Proc. Blazar Continuum Variability, ASP Conf. Ser. 110, p. 17
- Morris S.L., Stocke J.T., Gioia I.M., et al., 1991, ApJ 380, 49
- Padovani P., Giommi P., 1995, ApJ 444, 567
- Penston M.V., Cannon R.D., 1970, Roy.Obs.Bull. 159, 85
- Perlman E.S., Stocke J.T., 1993, ApJ 406, 430
- Pesce J.E., Urry C.M., Maraschi L., et al., 1997, ApJ, in press
- Sambruna R., Maraschi L., Urry C.M., 1996, ApJ 463, 444
- Simonetti J.H., Cordes J.M., Heeschen D.S., 1985, ApJ 296, 46
- Smith A.G., Nair A.D., Leacock R.J., Clements S.D., 1993, AJ 105, 437
- Stickel M., Padovani P., Urry C.M., Fried J., Kühr H., 1991, ApJ 374, 431
- Stocke T.J., Liebert J., Schmidt G., et al., 1985, ApJ 298, 619
- Takalo L.O., 1997, Reflections from the OJ-94 project. In: Miller H.R., Webb J.R., J.C. Noble (eds.) Proc. Blazar Continuum Variability, ASP Conf. Ser. 110, p. 70
- Urry C.M., Padovani P., 1995, PASP 107, 803
- Wagner S.J., Sanchez-Pons F., Quirrenbach A., Witzel A., 1990, A&A 235, L1
- Wagner S.J., Witzel A., 1995, ARA&A 33, 163
- Wagner S.J., Witzel A., Heidt J., et al., 1996, AJ 111, 2187
- Wagner S.J., Takahashi T., Dietrich M., et al., 1997, ApJL, in press
- Wurtz R., Stocke J.T., Yee H.K.C., 1996, ApJS 103, 109
- Wurtz R., Stocke J.T., Ellingson E., Yee H.K.C., 1997, ApJ 480, 547
- Xie G.Z., Zhang, Y.H., Li K.H., et al., 1996, AJ 111, 1065

This article was processed by the author using Springer-Verlag L^AT_EX A&A style file L-AA version 3.